



Analysing Geothermal Heat Exchangers Using Comsol Non-Isothermal Pipe Flow Model

Mohammed A. Atiya¹, Ali Naser Hussien², Azher M. Abed³,
Philippe Mandin⁴ and Farkad Ali Lattieff^{5*}

¹ Department of Biochemical Engineering, Al-Khwarizmi College of Engineering, University of Baghdad, Baghdad, Iraq

² Department of Biomedical Engineering, University of Technology, Baghdad, Iraq

³ Department of Air Conditioning and Refrigeration, Al-Mustaqbal University, Babylon, Iraq

⁴ Institut de Recherche Dupuy de Lôme, Université de Bretagne Sud, IRDL UMR CNRS 6027, Lorient 56100, France

⁵ Department of Energy Engineering, College of Engineering, University of Baghdad, Baghdad, Iraq

Corresponding Author's Email: Farkad.ali@coeng.uobaghdad.edu.iq

(Received 19 October 2024; Revised 9 January 2025; Accepted 19 January 2025; Published 1 March 2025)

<https://doi.org/10.22153/kej.2025.01.001>

Abstract

Earth–air heat exchangers (EAHE) hold great promise for reducing typical air conditioning systems' energy consumption whilst preserving high indoor comfort. The present analyses a 3D model using COMSOL Multiphysics software for a geothermal heat exchanger to examine the thermal behavior along the piping system. The experimental findings of the real EAHE in Baghdad City during January and June are transferred into the nonisothermal pipe flow interface for modeling temperature, velocity and pressure distributions along the piping system. The temperature variation of subsurface soil and the radial temperature distribution around the pipe are modeled into the heat transfer interface. The magnitude of heat flux is also computed in different times along the pipe. The effects of the continuous operation of EAHE on the output temperature and on the soil temperature around the pipe are also considered. The model's output demonstrates that the air temperature rise in January is 10 °C, whereas the air temperature drop is 14 °C in June. The effect of extracted/absorbed heat transfer from/to air in pipes is extended up to 0.7 m in the radial direction of the soil surrounding pipes due to continuous airflow in EAHE.

Keywords: geothermal energy; sandy soil; earth heat exchanger; COMSOL; thermal analysis

1. Introduction

As the global economy continues to expand, more energy is being used to power conventional air conditioning and refrigeration equipment in buildings and industries. The primary mechanism for transferring heat between various media is the heat exchanger [1-3]. One of the primary uses of heat exchangers is air conditioning, and their shapes and designs vary according to the advantages they offer [4-6]. Earth–air heat exchanger (EAHE) is a pipe extended in the earth at a few meters depth where the soil is far from the weather fluctuations in winter and summer. Moreover, the temperature is

moderate, and its variation is very small; thus, it is a good means for heating in winter and cooling in summer. A further advantage is that it is a potential technology for lowering the quantity of electricity that is consumed. Recently, the application of the EAHE has extended to a wide range of uses such as markets, swimming pools, housing and commercial buildings, industry and agriculture applications [7-10].

Various studies outline a design technique for improving the heat transferred between the interior buried pipes and the surrounding soil [11-14]. Numerous advances in numerical simulation models have been achieved to predict the performance of horizontally laid-out earth air heat



exchangers [15–18]. Mohammed H. Ali et. al. presented a MATLAB/Simulink model to forecast soil temperature distribution and effective EAHEs [19]. They created this model based on their experimental results to prove the multiple–single pipe EAHE is better in terms of pressure loss and cooling potential compared with the twisted–single pipes one. In addition, they claimed that their model could be used to estimate the soil temperature at any depth. Hussein, A.N., conducted a numerical study on EAHE for different input temperatures on hot days in Baghdad City and considered the effect of soil thermal saturation on the lessening of air cooling [20].

Performing an extensive 3D analysis of EAHE performance is difficult, and various effective parameters increase the use of computational fluid dynamics (CFD)-based simulation software. This software provides simple, powerful solution methods.

Numerical simulation depends on experimental measurements demonstrated by Flaga-Maryanczyka et al., [21] EAHE for passive ventilation in the winter of Poland and the simulation performed by CFD software package of ANSYS FLUENT. The study showed a satisfactory approximation between numerical and value with the average difference does not exceed 1.7 °C.

Ramirez-Davila et al., [22] conducted a comparative analysis study to determine the performance of the EAHE system in sandy, salty and clay soils in Ciudad Juarez, Mexico City, and Merida, respectively. They used a CFD code to model the system. The simulation results indicated that the average air temperature decreases by 6.6 °C and 3.2 °C in summer for Ciudad Juarez and Mexico City, respectively, and rises by about 2.1 °C and 2.7 °C in winter for Ciudad Juarez and Mexico City, respectively. For Merida, the increase of air temperature is 3.8 °C. The study proved the suitability of the EAHE for extreme and moderate weather temperatures.

A simulated study introduced by Naqash et. al. [23] using a COMSOL Multiphysics as a CFD tool provided valuable results about the advantages of using EAHE, especially in severe hot or cold climates. The study was validated by a broad field test, designed for Islamabad's soil properties and climatic conditions. The results concluded that the EAHE can work as a boosting system for air-conditioning devices and decreases the electric energy cost by about 30% to 60%.

Baghdad records the highest temperatures during summer, and the need for electrical energy for cooling purposes increases. Temperatures drop during winter, especially at night, so using EAHE as

a renewable energy source to meet the increasing need for energy is very appropriate. In the present paper, the system of EAHE is designed and implemented practically as an experimental test system. The practical measurements such as temperatures of air and soil, and air pressure and velocity, are taken and transferred as input data of COMSOL Multiphysics software, to obtain a complete analysis of the system. The aims of the paper can be summarised as follows:

1. Create a comprehensive 3D modelling of the air and the soil surrounding the EAHE system using a CFD code COMSOL Multiphysics
2. Calculate the air temperature difference through the EAHE in summer and winter due to heat transfer, which is the purpose of using EAHE
3. Evaluate the effect of continuous operation of EAHE on its performance and the soil temperature around the pipe.

2. System Description

The schematic of the experimental EAHE prototype drawn by COMSOL Multiphysics software is shown in Fig. 1. This prototype, which is designed to cover the test of various operating air conditions in summer and winter, is fabricated at the University of Baghdad, Iraq, and consists of a centrifugal blower of 300-watt capacity and a series of PVC pipes with 0.1m diameter and 0.005 m thickness. The PVC pipes are extended vertically downward to a four-meter depth and then extended horizontally to three pipe segments; two of them are parallel, 8 m long and connected by a third segment of 2 m length. The last part of the PVC pipes that completes the open circuit EAHE is the 4 m length of vertical upward pipe. The total pipe length is 26 m; 18 m forms the horizontal buried part, and 8 m form the two equal and parallel vertical downward and upward parts. The velocity of the ambient air can be controlled by a variable opening gate installed at the entrance air inlet of the blower. The outlet air enters a caravan installed to monitor the air condition results.

The air temperature at the inlet, outlet and along the EAHE and the air velocity, in addition to the soil temperature at different locations near the EAHE, are the main important parameters, that must be measured to obtain the required data for numerical simulation. For this object, seven thermocouples (type K) are distributed at equal distances, to measure the air temperature at the inlet, outlet and inside the pipe (T_{in} , T_1 , T_2 , T_3 , T_4 , T_5 and T_{out}). Another set of five thermocouples is located at

different levels in the soil to measure the disturbed and undisturbed temperatures of the soil (T_6 , T_7 , T_8 , T_9 and T_{soil}). All thermocouples are connected to a data logger of 32 channels. Type CKT4000 series multichannel temperature recorder uses 32-bit high-speed CPU for data processing and records every 60 s. Pressure drop does not affect heat exchange

during the EAHE, so it is not considered in the experimental measurement. A computer collects and processes the measurement data acquired by the data logger. The air velocity is measured by a vane-type anemometer at the pipe exit and controlled manually. The overall system installation is shown in Figure 1.

Table 1,
Experimental findings of EAHE on the first day of operation

Month	Time (hours)	$T_{inlet\ air} (^\circ C)$	$T_{outlet\ air} (^\circ C)$	$T_{soil} (^\circ C)$ at 4 m depth
January	12	10	21.5	25.7
June	14	46	32	23.9

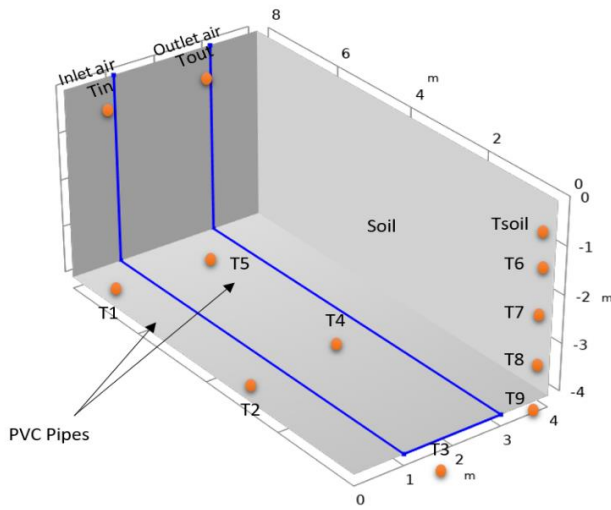


Fig. 1. Experimental earth heat exchanger prototype

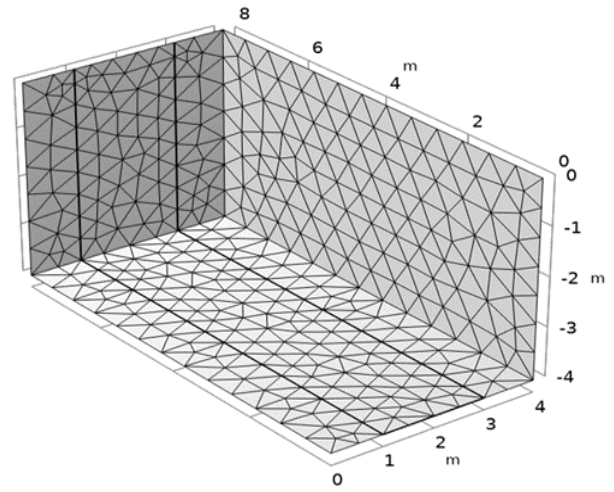


Fig. 2. Piping system and soil geometry mesh in COMSOL

3. Model Explanation

The Nonisothermal Pipe Flow CFD tool is used to model the temperature, velocity and pressure fields in EAHE pipes. This model uses functions and experimental findings to represent the actual operating situations. The Nonisothermal Pipe Flow interface constructs and solves the temperature and fluid flow equations for the soil and pipes system, where 3D lines represent the geometry. Figure 2 indicates the piping system and soil geometry mesh is created by COMSOL Multiphysics software. Time-dependent surface temperature matches normal conditions of Baghdad City temperature fluctuations. However, the ambient temperature above the surface may drop to the lowest temperature of 8 °C during January and the highest one of 43 °C during June. The physical properties of air as a function of temperature are directly available from the software’s built-in material library.

The transient heat conduction in 2D (r: radial and x: axial) coordinate is [24].

$$\frac{\rho c_s}{k_s} \left(\frac{\partial T}{\partial t} \right) = \frac{\partial^2 T}{\partial x^2} + \frac{\partial}{\partial r} \left(r \frac{\partial T}{\partial r} \right), \quad \dots(1)$$

where ρ is the soil density, c_s is the soil specific heat capacity and k_s is the soil coefficient of thermal conductivity.

The air in EAHE absorbs/releases heat rate in winter/ summer according to Paepe and Janssens [25]:

$$Q = \dot{m}_a c_p (T_{out} - T_{in}), \quad \dots(2)$$

where \dot{m}_a , c_p , T_{out} and T_{in} are air mass flowrate, air specific heat capacity, outlet air and inlet air temperature, respectively. This heat rate takes a positive and negative sign in winter and summer, respectively, according to the temperature difference sign.

This heat rate exchanges with the soil surrounds the pipe and computed according to Paepe and Janssens [25].

$$Q = hA\Delta T_{LM}, \quad \dots(3)$$

where h is the convective heat-transfer coefficient, A is the pipe surface area and ΔT_{lm} is the mean logarithm of temperature difference and computed as [25].

$$\Delta T_{lm} = (T_{out} - T_{in}) / \ln \left[\frac{(T_{wall} - T_{in})}{(T_{wall} - T_{out})} \right] \quad \dots(4)$$

From Eqs. (2) and (3) and eliminate Q_h with substitute Eq. (4), the T_{out} is computed as follows:

$$T_{out} = T_{wall} - (T_{wall} - T_{in}) \exp(-hA/\dot{m} c_p) \quad \dots(5)$$

The heat-transfer coefficient by convection h is computed as Holman [26]:

$$h = Nu * k_{air} / d, \quad \dots(6)$$

where k_{air} is the conductive heat transfer of air, d is the diameter of the pipe and Nu is the Nusselt number computed by Singh [27] and Lemmon and Jacobsen [28]:

$$Nu = 0.023 * Re^{0.8} Pr^n \quad \dots(7)$$

The index n is a constant of 0.4 or 0.3 corresponding to heating or cooling operation, respectively. Re and Pr that appear in above Eq. are Reynolds and Prandtl numbers, respectively, and can be computed as [24]:

$$Re = \rho_{air} v d / \mu, \quad Pr = \mu c_p / k_{air} \quad \dots(8)$$

where ρ_{air} , v and μ are respectively the density, velocity and absolute viscosity of the air.

The air pressure drop in the EAHE is due to friction, with a smooth inner pipe wall assumption (Cengel and Cimbala, 2014) [29]:

$$\Delta p = f \rho_{air} \frac{L v^2}{d} \quad \dots(9)$$

where f and L are the friction factor and pipe length respectively, and f is calculated as [29]:

$$f = 64 / Re \quad \text{if} \quad Re < 2300 \quad \dots(10)$$

and

$$f = (1.82 \log Re - 1.64)^{-2} \quad \text{if} \quad Re \geq 2300 \quad \dots(11)$$

The experimental measurements reveal that the Reynolds number is much greater than 2300.

The experimental measurements reveal that the Reynolds number is much greater than 2300.

The pressure drop due to elbows can be calculated as [29].

$$\Delta p = K \rho_{air} \frac{v^2}{2}, \quad \dots(12)$$

where K is the loss coefficient of the elbow and equal to 0.9.

The power needed for air-flow can be calculated as [29]:

$$P_f = \Delta p * \dot{V} \quad \dots(13)$$

Table 2,
Model input

Notation	k	ρ	C_p
pipe	0.16	1380	900
soil	1.5	1742	1175

4. Results and Discussion

A numerical modeling of EAHE using COMSOL Multiphysics software based on experimental measurements is used. The measurements are conducted in summer and winter. The ambient temperature variation along the year and the temperature variation against the depth underground in January (winter) and June (summer) are shown in Figure 3 a and b, respectively, whereas the temperature variation with depth of 3D pipe–soil configuration without airflow is indicated in Figure 4 for the two months. The temperatures converge with increasing depth despite the different ambient temperatures through the January and June months. By contrast, the temperature of the earth’s surface and the nearest subsurface are affected by the hourly variation of ambient temperatures.

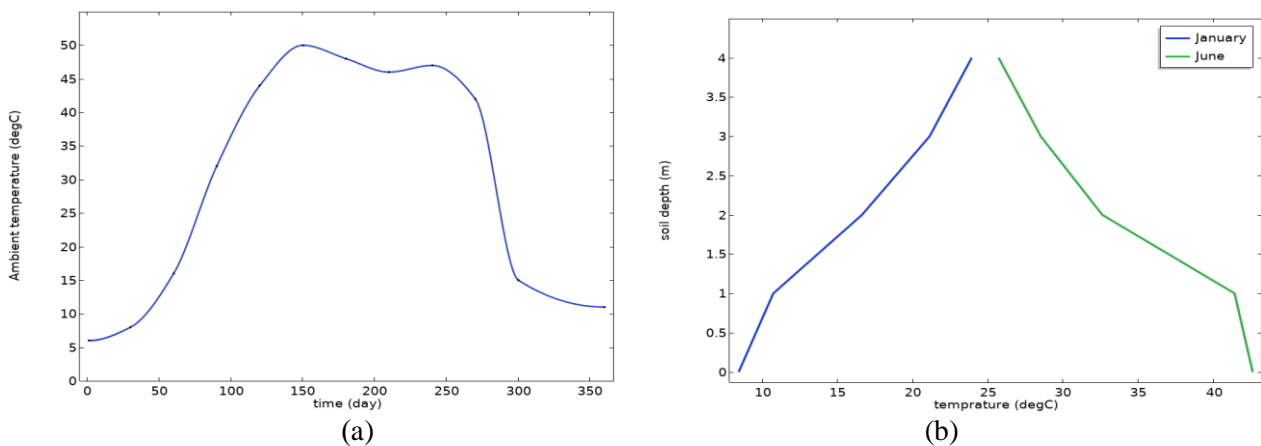


Fig. 3. (a) Variation of ambient temperature and (b) Soil depth temperature during the coldest (January) and hottest (June) months

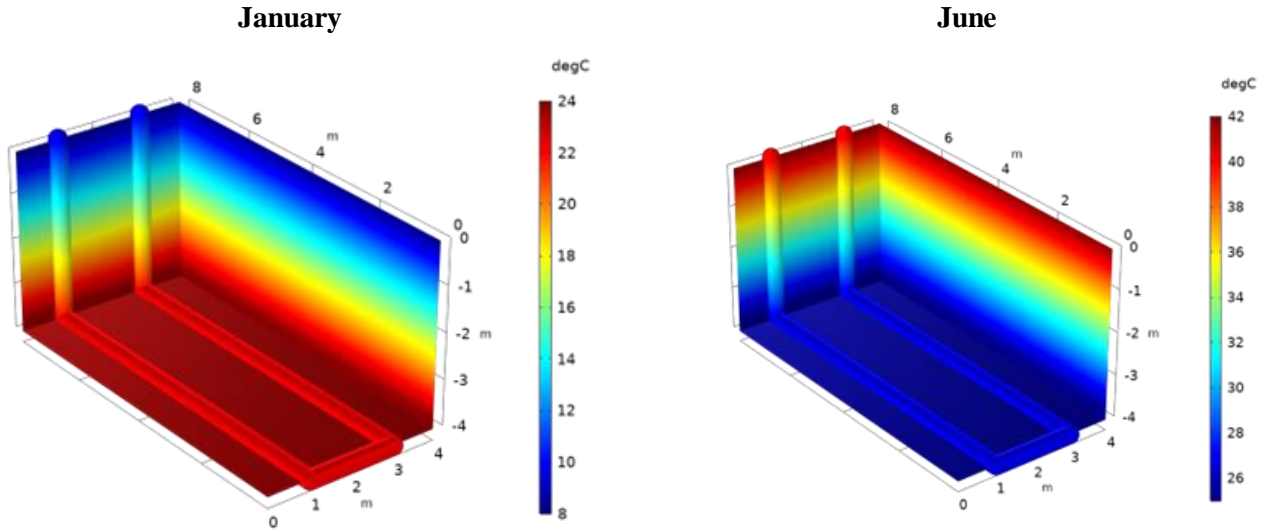
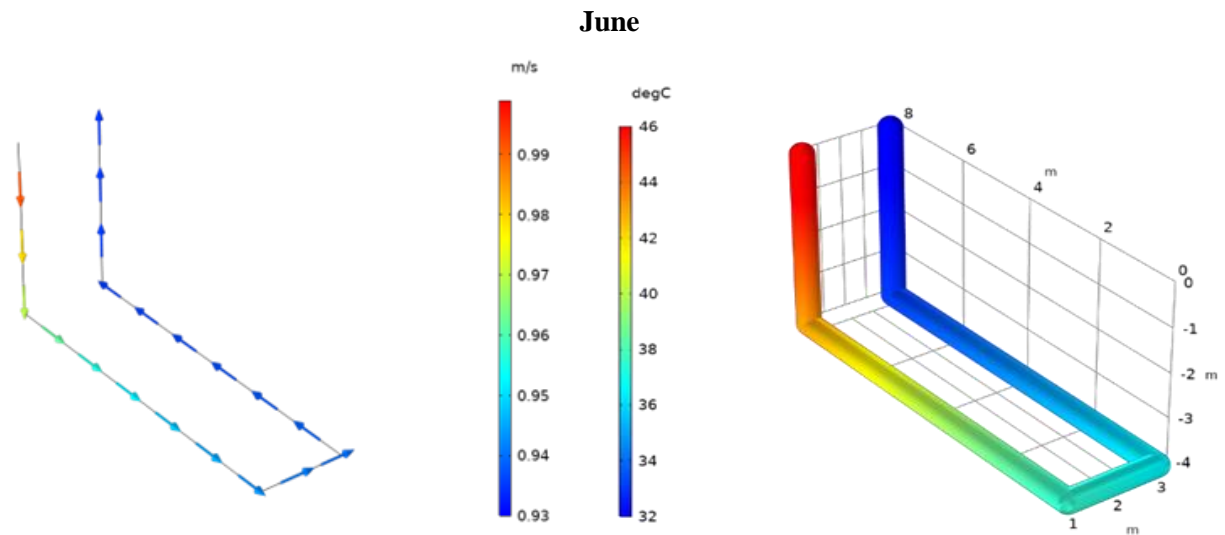


Fig. 4. Profiles of soil depth and EAHX temperatures when no air flow rate ($u = 0$ m/s)

The average air velocity vectors and the air temperature variation inside the pipe during January and June are illustrated in Figure 5. The blower is placed at the pipe inlet, and the average air velocity changes from the inlet to the outlet from 1 m/s to 1.06 m/s, in January, and from 1 m/s to 0.93 m/s in June. This increase in average air velocity in January and decrease in June can be attributed to the effect of air density variation, that is, the cold air of high density goes down at the inlet and the hot air of low density goes up at the outlet. Moreover, the direction of the air being pushed by the blower

during winter leads to an increase in the average air velocity from the inlet to the outlet. On the contrary, the blower pushes the hot air down at the inlet and the cold air up at the outlet, opposite to the density gradient of the air, so the average air velocity decreases from the inlet to the outlet in summer. The increase of the air temperature by 10 °C as a heating effect at 2 am, in the first day of operation in January and its decrease by 14 °C as a cooling effect at 2 pm on the first day of operation in June, are presented in Figure 5.



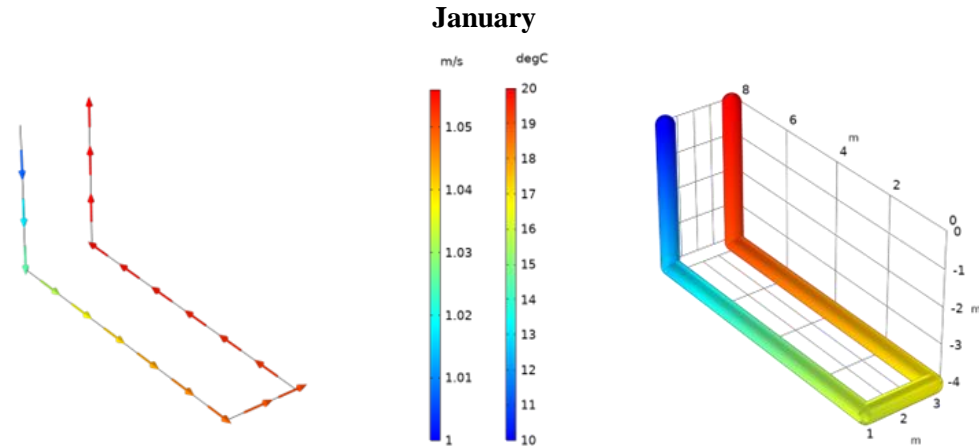


Fig. 5. Variation of average air velocity and air temperatures along the EAHX pipes during June and January

Figure 6 shows similar temperature changes along the EAHE pipe. The air temperature drop on June 14 °C is higher than that of January of 10 °C due to the high-temperature difference between the inlet air temperature of 46 °C and the soil undisturbed temperature of 23.9 °C in June. This difference is lower in January, which is 10 °C for inlet air and 25.7 °C for undisturbed soil. These differences lead to high heat flux transferred when high-temperature differences occur, and vice versa.

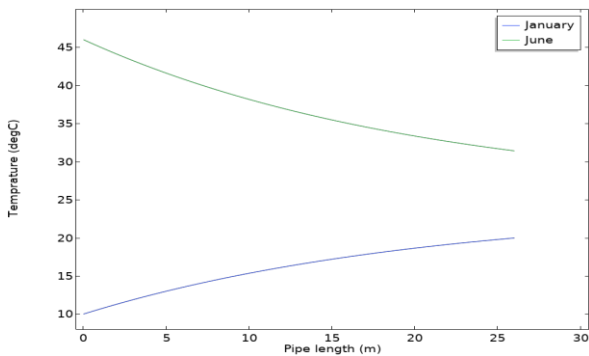


Fig. 6. Air temperature profile along the EAHX pipes during June and January

Figures 7 and 8 show the heat flux variation along the pipe between the air and the soil for January and June, respectively. The hourly ambient temperatures are measured during the four days of EAHE system operation. For January, the times of 2:00 am and 12:00 pm are selected as a case study of heat flux changes, as shown in Figure 7, whereas for June, 8 am and 2 pm are selected, as illustrated in Figure 8.

The nonisothermal model is used to calculate the heat losses/stored in the soil during the continuous operation of the four consecutive days. The positive and negative parts of heat flux refer to the direction of heat from soil to air and from air to soil, respectively, as presented in Figure 7. By contrast, the air cooling and heating are represented by positive and negative heat fluxes, respectively, for June, as shown in Figure 8. However, the maximum heat flux occurs at the maximum temperature difference between the soil and air, that is, at 2:00 am in January and at 2:00 pm in June. This difference in temperature between the air and soil is higher than that at 12:00 pm in January and 8:00 am in June, especially on the first day of operation, and then gradually decreases in the three other consecutive days due to the continuous heat losses from the soil in January and continuous heat gain to the soil in June. The maximum heat fluxes in January at 2:00 am along the four consecutive days are 51.5, 34.7, 32.2 and 30.2 W/m^2 , whereas the maximum heat flux at 12:00 pm does not exceed 8.4 w/m^2 for the same days. The peak heat flux values in June occur at 2:00 pm and are 41.2, 37.7, 36.4, and 35.7 w/m^2 for the four consecutive days, whereas the maximum heat flux values reach 15.2 w/m^2 at 8:00 am. The heat flux values at the first and last four meters of the vertical pipe length, and the temperature of the soil increases gradually with increasing the depth in January and on the contrary in June. Figs. 7 and 8 show that the heat transfer can be changed in the direction from the negative at 12:00 pm when the air is cooled by the value exceeded to about 20.3 W/m^2 in January and at 2:00 am in June when the air is heated to about 14 W/m^2 .

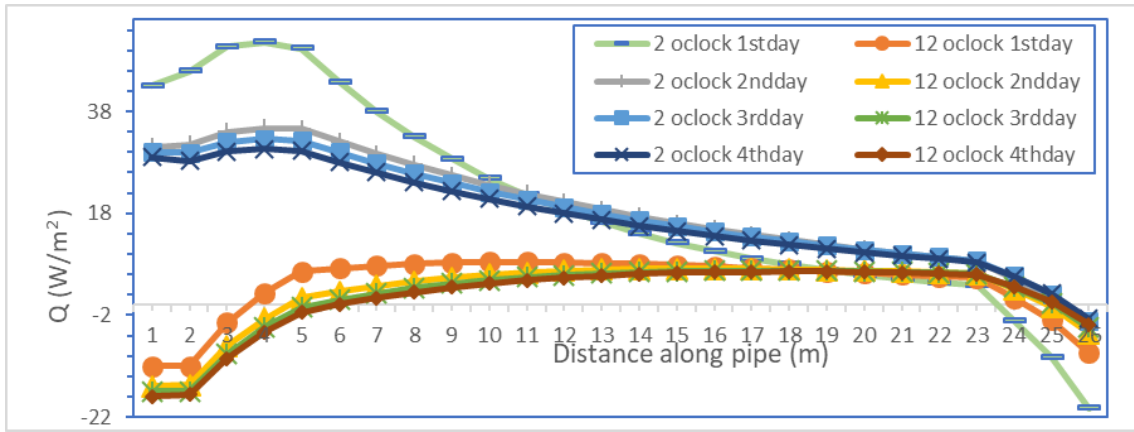


Fig. 7. Variation of heat flux along the EAHE pipes in January

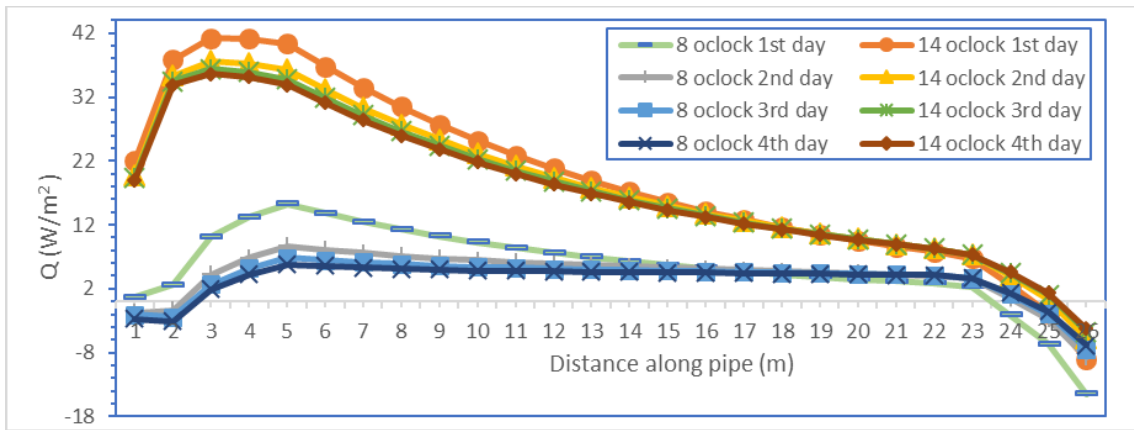
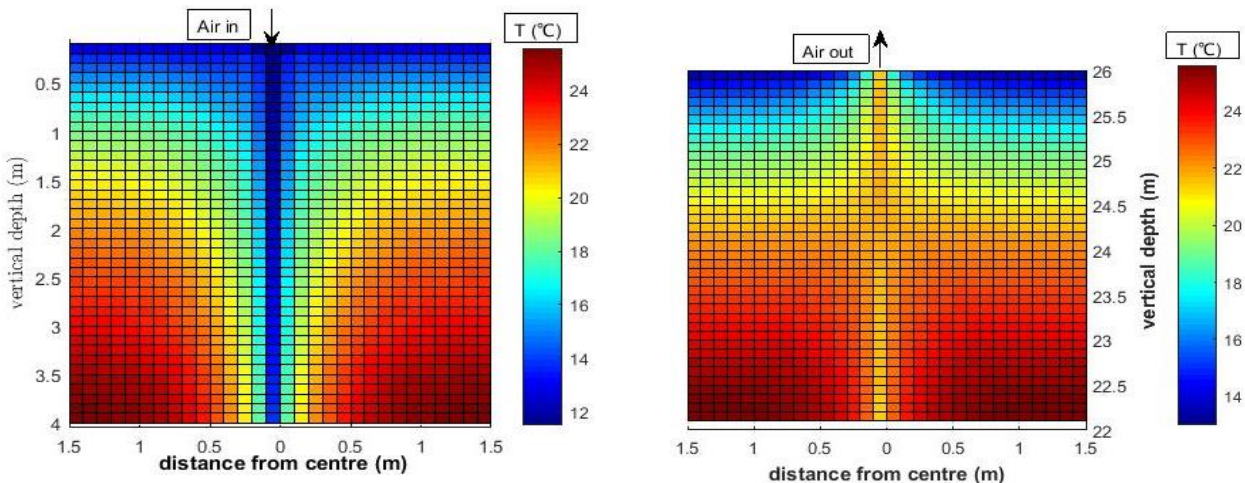


Fig. 8. Variation of heat flux along the EAHE pipes in June.

The temperature distributions along the vertical and the horizontal parts of EAHE are illustrated in Figure 9 and 10. On the third day of the continuous operation at 8:00 pm in January, Fig. 9 shows the effect of heat transfer from the soil to the buried pipe inside it. The disturbed soil temperature variations form a truncated cone of the base radius equal to about 0.7 m, at the inlet of the horizontal part and

about 0.3 m at the end of it, after two days and 20 hours in January. The disturbed temperature near the pipe at the beginning and the end of the horizontal part are to 18°C and 22 °C, respectively, in January whereas the undisturbed soil temperature is 25.7 °C.



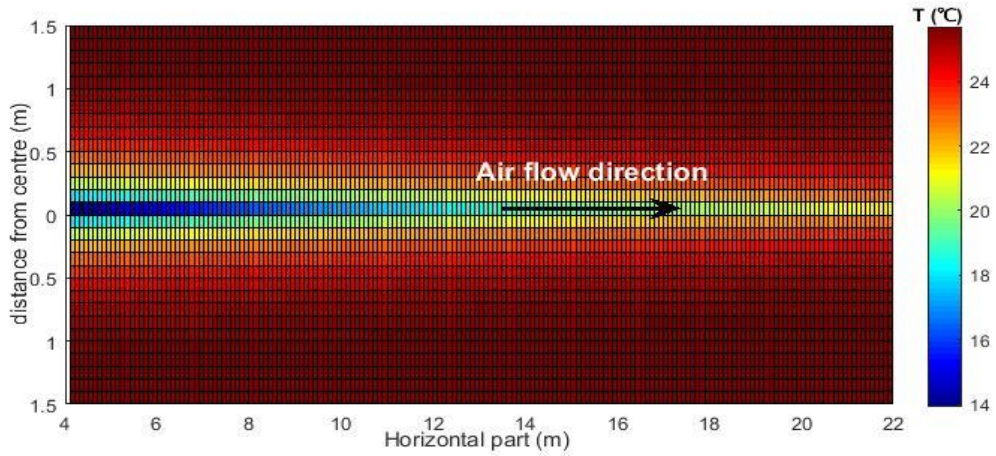


Fig. 9. Temperature variation of air in the pipe and the soil around it at 8:00 pm on the third day of continuous operation in January

Figure 10 illustrates the temperature changes for the piping system and the surrounding soil in June after two days and 15 h of continuous operation. The disturbed soil temperature at the beginning and

the end of the horizontal part are 34.5 °C and 27 °C, respectively, with 23.9 °C of undisturbed soil temperature.

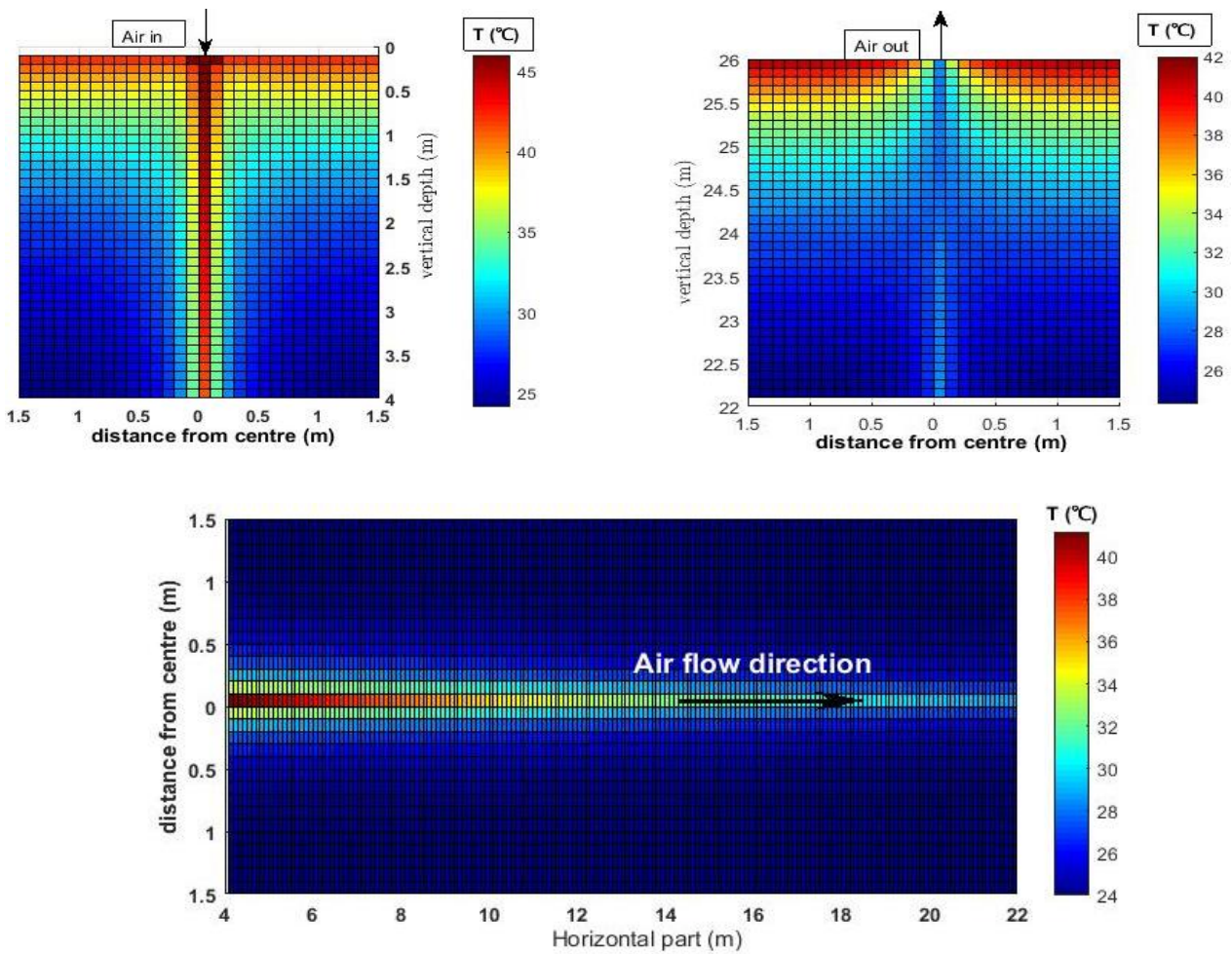


Fig. 10. Temperature variation of air in the pipe and the soil around it at 3:00 pm on the third day of continuous operation in June

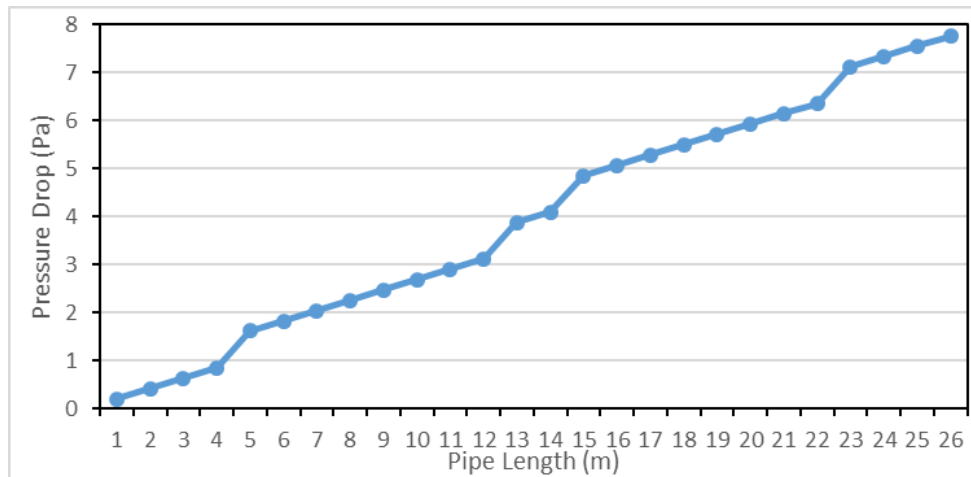


Fig. 11. Pressure drop along the EAHE pipe

The formation of these regions around the pipe reduces the temperature differences between the soil and the air, which leads to a decrease in the air heating and soil temperature in January, a decrease in the air cooling and an increase in the soil temperature in June. Moreover, these figures show the effects of the soil temperature gradient in the vertical parts and the influence of continuous operation on the EAHE system performance. The temperature distribution in vertical parts of the EAHE system indicates the cooling of air in the vertical part before the pipe outlet in January and the heating of air in this part in June because the soil temperature is close the ambient air temperature; therefore, this part decreases the benefit of EAHE, and the pipe in this part must be completely insulated.

The pressure drop along the pipe due to friction and due to 4 elbows is shown in Fig. 11. The pressure drop due to friction increases by 0.214 Pa for each meter of pipe length, and the pressure drop due to the elbows increases by 0.549 Pa for each elbow the pressure drop at the exit, that is, 7.77 Pa represents the total pressure drop along the pipe. This value is multiplied by the air discharge as explained by Eq. (13) to calculate the power losses due to friction and elbows, which is 0.06 W.

5. Conclusions

The use of EAHE is a satisfactory, clean choice for cooling/heating air or decreasing the cost of traditional energy systems when it is invested wisely. Nonisothermal analysis or the consideration of the soil temperature variation achieves higher accuracy and more reality in studying the

performance of the EAHE system. The continuous operation or continuous air passing through the pipes of EAHE reduces the air heating in winter and air cooling in summer. The vertical part of the pipe at the outlet must be surrounded with low thermal conductive material to lessen the disadvantage of heat transfer in this part due to temperature variation toward the ground surface.

Nomenclature

A	m^2	cross-section area of the pipe
A_s	m^2	surface area of the pipe wall
C_p	$J/kg \cdot ^\circ C$	heat capacity at constant pressure
d_h	m	hydraulic pipe diameter
F	N/m^3	volume force (gravity)
h	$W/m^2 \cdot ^\circ C$	heat transfer coefficient
k	$W/m \cdot ^\circ C$	thermal conductivity
p	N/m^2	pressure
q_{cond}	W/m^2	conductive heat flux
q_{conv}	W/m^2	convective heat flux
Q	W/m^2	heat source
r_i	m	wall inner radius
r_o	m	wall outer radius
T	$^\circ C$	temperature
u	m/s	fluid velocity
ρ	kg/m^3	density
∇		gradient operator

References

- [1] Mutlak FA-H. Construction and performance study of a solar - powered hybrid cooling system in Iraq. *Iraqi Journal of Physics*. 2019, 24, 11(21):91-101.
- [2] Hanaa Abdulhussein, Ahmed M. Abdulhadi. Impact of Heat Transfer and Inclined MHD on A Non-Uniform Inclined Asymmetrical Channel with Couple Stress Fluid Through A Porous Medium. 2023, *Iraqi Journal of Science*, 64(9), 4580-4599.
- [3] Ahmed A. K., & N. S. Kadhim. Analysis of the performance of a cooling system (Refrigerator) operating with a thermoelectric cooling system used to preserve crops and agricultural products. 2024, 55(5), 1766-1773.
- [4] Majeed Hameed, V., & Ali Hussein, M. Studying the Performance of Refrigeration Units Powered by Solar Panel. *Iraqi Journal of Chemical and Petroleum Engineering*, 2013, 14(1), 39-46.
- [5] Ahmed Abd Mohammed Saleh and Ali Reyadh Shabeeb. Theoretical Prediction of Optimum Chilled Water Distribution Configuration in Air Conditioning Terminal Unit. *Al-Khwarizmi Engineering Journal*, 2019, 14(2), 137-146.
- [6] Yasser Abdul Lateef Ghani and Abdul Hadi N. Khalifa. Energy, Exergy and Anergy Analysis of Vertical Split Air Conditioner under Experimental ON-OFF Cycling. *Journal of Engineering*, 2019, 25(7), pp. 1–20.
- [7] Amin Shahsavari and Neda Azimi b. Performance evaluation and multi-objective optimization of a hybrid earth-air heat exchanger and building-integrated photovoltaic/thermal system with phase change material and exhaust air heat recovery. *Journal of Building Engineering* Volume 90, 1 August 2024, 109531.
- [8] Lund, J.W.; Boyd, T.L. Direct utilization of geothermal energy 2015 worldwide review. *Geothermics* 2016, 60, 66–93.
- [9] Zhou, Y.; Bidarmaghzi, A.; Narsilio, G.; Aye, L. Heating and Cooling Loads of a Poultry House in Central Coast, NSW, Australia. In *Proceedings of the World Sustainable Built Environment Conference 2017, Hong Kong, China, 5–7 June 2017*
- [10] Sehli A, Hasni A, Tamali M. The potential of earth-air heat exchangers for low energy cooling of buildings in South Algeria. *Energy Procedia*. 2012; 18:496–506.
- [11] D’Agostino, D.; Greco, A.; Masselli, C.; Minichiello, F. The employment of an earth-to-air heat exchanger as pre-treating unit of an air conditioning system for energy saving: A comparison among different worldwide climatic zones. *Energy Build*. 2020, 229, 110517.
- [12] Dong Zhang, Jingrui Zhang, Chunyang Liu, Chengtao Yan, Jinchao Ji, Zhoujian An. Performance measurement and configuration optimization based on orthogonal simulation method of earth-to-air heat exchange system in cold-arid climate. *Energy and Buildings* Volume 308, 1 April 2024, 114001.
- [13] Jinxin Xiao, Qiang Wang, Xiaoyan Wang, Yixin Hu, Yanfei Cao, Jianming Li. An earth-air heat exchanger integrated with a greenhouse in cold-winter and hot-summer regions of northern China: Modeling and experimental analysis. *Applied Thermal Engineering* Volume 232, September 2023, 120939.
- [14] Lattieff FA, Atiya MA, Lateef RA, Dulaimi A, Jweeg MJ, Abed AM, Mahdi JM and Talebizadehsardari P (2022), Thermal analysis of horizontal earth-air heat exchangers in a subtropical climate: An experimental study. *Front. Built Environ.* 8:981946. doi: 10.3389/fbuil.2022.981946.
- [15] Aslam Bhutta MM, Hayat N, Bashir MH, Khan AR, Ahmad KN, Khan S. CFD applications in various heat exchangers design: A review. *Appl Therm Eng.* 2012;32(1):1–12.
- [16] Wu H, Wang S, Zhu D. Modelling and evaluation of cooling capacity of earth–air–pipe systems. *Energy Convers Manag.* 2007 May 1;48(5):1462–71.
- [17] Luca Cirillo, Adriana Greco, Claudia Masselli. Computational investigation on daily, monthly and seasonal energy performances and economic impact through a detailed 2D FEM model of an

- earth to air heat exchanger coupled with an air conditioning system in a continental climate zone. *Energy and Buildings* Volume 296, 1 October 2023, 113365.
- [18] Hamed Soroush, Soroush Entezari, Esmail Lakzian. Numerical investigation of serpentine earth-to-air heat exchanger for passive building heating systems by recovery criteria. *Sustainable Energy Technologies and Assessments* Volume 53, Part C, October 2022, 102728.
- [19] Mohammed H. Ali, Zoltan Kurjak, Janos Beke. Investigation of earth air heat exchangers functioning in arid locations using Matlab/Simulink. *Renewable Energy* Volume 209, June 2023, Pages 632-643.
- [20] Hussein, A.N., Numerical study on ground-air heat exchanger performance in a hot climate under different inlet air temperatures. *Journal of Energy Systems* 2023; 7(4): 315-326, DOI: 10.30521/jes.1097439.
- [21] Flaga M, Schnotale J, Radon J and Was K, 2014 Experimental measurements and CFD simulation of a ground source heat exchanger operating at a cold climate for a passive house ventilation system. *Energy and Buildings*. pp 562-570
- [22] Ramirez L, Xaman J A J, Alvarez G and Hernandez P 2014 Numerical study of earth to-air heat exchanger for three different climates. *Energy and Buildings*. pp 238-248
- [23] Naqash, M. T. Ouzzane, M and Harireche O. Modeling Earth-to-Air Heat Exchangers In Severe Climate. *Journal of Applied Science and Engineering* 2022, Vol. 26, No 1, Page 141-149 doi.org/10.6180/jase.202301_26(1).0015.
- [24] Çengel, Y. A. (2010) *Heat Transfer—A Practical Approach*. 4th ed. New York: McGraw-Hill,
- [25] De Paepe M, Janssens A. Thermo-hydraulic design of earth-air heat exchangers. *Energy Build.* 2003 May;35(4):389–97.
- [26] Holman, J.P. *Heat Transfer*. 10th Edition, McGraw-Hill, New York. (2009).
- [27] Singh SP. Optimization of earth-air tunnel system for space cooling. *Energy Convers Manag.* 1994 Aug 1;35(8):721–5.
- [28] Lemmon EW, Jacobsen RT. Viscosity and thermal conductivity equations for nitrogen, oxygen, argon, and air. *Int J Thermophys.* 2004;25(1):21–69.
- [29] Çengel, Y.A. and Cimbala, J.M. (2014) *Fluid Mechanics. Fundamentals and Applications*. 3rd Edition. McGraw-Hill, New York.

تحليل المبادلات الحرارية الأرضية ذي التدفق غير المتساوي الحرارة للأنابيب باستخدام برنامج الكومسل

محمد عبد عطية السراج¹، علي ناصر حسين²، أزهر محسن عبد³،
فيليب ماندين⁴، فرقد علي لطيف^{5*}

¹ قسم الهندسة الكيميائية الاحيائية، كلية الهندسة الخوارزمي، جامعة بغداد، بغداد، العراق

² قسم الهندسة الطبية الحيوية، الجامعة التكنولوجية، بغداد، العراق

⁴ قسم التكييف والتبريد، جامعة المستنقل، بابل، العراق

⁴ معهد البحوث دويوي دي لوم، جامعة بريتان سود، لوريان 56100، فرنسا

⁵ قسم هندسة الطاقة، كلية الهندسة، جامعة بغداد، بغداد، العراق

* البريد الإلكتروني : Farkad.ali@coeng.uobaghdad.edu.iq

المستخلص

تتمتع المبادلات الحرارية الأرضية الهوائية (EAHE) بعود كبيرة في تقليل استهلاك الطاقة لأنظمة تكييف الهواء النموذجية مع الحفاظ على الراحة الداخلية العالية. اعتمدت الدراسة الحالية تحليل نموذج ثلاثي الأبعاد باستخدام برنامج COMSOL Multiphysics لمبادل حراري أرضي لفحص السلوك الحراري على طول نظام الأنابيب. تم نقل النتائج التجريبية لمبادل حراري أرضي هوائي حقيقي في مدينة بغداد خلال شهري يناير ويونيو إلى واجهة تدفق الأنابيب غير المتساوية الحرارة لنمذجة توزيع درجات الحرارة والسرعة والضغط على طول نظام الأنابيب. تم نمذجة التغير في درجة حرارة التربة تحت السطحية وتوزيع درجة الحرارة الشعاعية حول الأنبوب في واجهة نقل الحرارة. وتم أيضًا حساب حجم تدفق الحرارة في أوقات مختلفة على طول الأنبوب. تأخذ الدراسة في الاعتبار تأثيرات التشغيل المستمر لمبادل حراري أرضي هوائي على درجة حرارة الإخراج ودرجة حرارة التربة حول الأنبوب. أظهرت نتائج النموذج أن ارتفاع درجة حرارة الهواء في يناير هو 10 درجات مئوية، في حين أن انخفاض درجة حرارة الهواء هو 14 درجة مئوية في يونيو. يمتد تأثير نقل الحرارة المستخرجة/المتصدة من/إلى الهواء في الأنابيب حتى 0.7 متر في الاتجاه الشعاعي للتربة المحيطة بالأنابيب بسبب تدفق الهواء المستمر في EAHE.